



Published in final edited form as:

Cell Rep. 2016 April 5; 15(1): 158–170. doi:10.1016/j.celrep.2016.03.012.

Single cell lineage tracing reveals that oriented cell division contributes to trabecular morphogenesis and regional specification

Jingjing Li¹, Lianjie Miao¹, David Shieh¹, Ernest Spiotto¹, Jian Li², Bin Zhou³, Antoni Paul¹, Robert J. Schwartz⁴, Anthony B. Firulli⁵, Harold A. Singer¹, Guoying Huang², and Mingfu Wu^{1,*}

¹Center for Cardiovascular Sciences, Albany Medical College, Albany, NY 12208

²Key Laboratory of Molecular Medicine, Ministry of Education, Fudan University, Shanghai, China, 200032

³Department of Genetics, Albert Einstein College of Medicine of Yeshiva University, Bronx, New York 10461, USA

⁴Biology and Biochemistry, University of Houston, Houston, TX 77204-5001, USA

⁵Riley Heart Research Center, Indiana University, Indianapolis, IN 46202, USA

Summary

The cardiac trabeculae are sheet-like structures extending from the myocardium that function to increase surface area. A lack of trabeculation causes embryonic lethality due to compromised cardiac function. To understand the cellular and molecular mechanisms of trabecular formation, we genetically labeled individual cardiomyocytes prior to trabeculation via the brainbow multicolor system, and traced and analyzed the labeled cells during trabeculation by whole-embryo clearing and imaging. The clones derived from labeled single cells displayed four different geometric patterns that are derived from different patterns of oriented cell division (OCD) and migration. Of the four types of clones, the inner, transmural, and mixed clones contributed to trabecular cardiomyocytes. Further studies showed that perpendicular OCD is an extrinsic asymmetric cell division that putatively contributes to trabecular regional specification.

Furthermore, N-Cadherin deletion in labeled clones disrupted the clonal patterns. In summary, our data demonstrate that OCD contributes to trabecular morphogenesis and specification.

*Correspondence to Mingfu Wu, Ph.D., ME616, 43 New Scotland Ave, MC8, Cardiovascular Science Center, Albany Medical College, Albany NY 12208, wum@mail.amc.edu, Phone: 518-262-5795, Fax: 518-262-8101.

Publisher's Disclaimer: This is a PDF file of an unedited manuscript that has been accepted for publication. As a service to our customers we are providing this early version of the manuscript. The manuscript will undergo copyediting, typesetting, and review of the resulting proof before it is published in its final citable form. Please note that during the production process errors may be discovered which could affect the content, and all legal disclaimers that apply to the journal pertain.

Competing interests

The authors declare no competing financial interests.

Author contributions

J. L., L.M., D. S., E. S., and M.W. performed the experiments and analyzed the data; M.W. designed experiments, and wrote the paper; A.P. helped the LCM experiments; J.L., GY. H., R.S., B.Z., A.B.F., and H.A.S. helped the projects.

Disclosures: None.

Introduction

Trabeculae are sheet-like structures that extend from the myocardium into the heart lumen to increase surface area, facilitating nutrient and gas exchange (Sedmera and Thomas, 1996). In mouse embryo, cardiac trabeculation is initiated at embryonic day 9 (E9.0), and by E10.5 long and thin trabeculae are formed. Subsequently, the trabeculae largely coalesce into the ventricular wall to thicken the compact myocardium. A lack of trabeculation causes embryonic lethality, while trabeculae failing to undergo compaction will result in left ventricular non-compaction (LVNC) cardiomyopathy (Breckenridge et al., 2007; Gassmann et al., 1995; Jenni et al., 1999; Pignatelli et al., 2003; Towbin et al., 2015; Weiford et al., 2004; Zhao et al., 2014). Approximately half a million Americans suffer from compromised heart function due to LVNC (Finsterer, 2010). Despite the fundamental functions of trabeculation, the molecular and cellular mechanisms underlying this process are not fully understood.

The cellular and molecular mechanisms of mammalian cardiac morphogenesis as a whole remain unclear, partly due to the multiple cell types involved, the intricate signaling interactions, and the challenges of analyzing the dynamic cellular behaviors during heart morphogenesis. Previously, sparse cell labeling via autonomous intragenic recombination has shown that myocardial precursors undergo two different phases of growth: dispersive growth along the venous-arterial axis of the cardiac tube, and oriented coherent cell growth, characterized by a lower level of intermingling (Meilhac et al., 2004; Meilhac et al., 2003). Virally labeled cells of the pre-cardiac mesoderm proliferate and form wedge-shaped colonies, with wider outer sides and narrower inner (luminal) sides (Meilhac et al., 2003; Mikawa et al., 1992a; Mikawa et al., 1992b). However, interpretations of these data are limited by the uncontrolled timing of single cell labeling, and imaging the labeled cells has been limited to the heart surface or two-dimensional analysis. To obtain a more comprehensive understanding of the mechanisms of trabecular morphogenesis, three-dimensional (3D) level imaging is required. Recently developed approaches including mosaic analysis with double markers and inducible multicolor labeling systems such as the brainbow system (Livet et al., 2007) have been used to determine early mesoderm progenitor specification (Chabab et al., 2016; Devine et al., 2014; Gupta and Poss, 2012; Lescroart et al., 2014). Applying such controllable inducible systems combined with 3D imaging to determine the cellular and molecular mechanisms underlying heart morphogenesis, especially trabeculation, has not yet been reported.

Previous work has shown that trabecular and compact cardiomyocytes display different features. Trabecular cardiomyocytes exhibit a lower proliferation rate and molecularly are more mature than cardiomyocytes of the compact zone (Sedmera et al., 2003). Differential expression patterns are well established between the trabecular and compact zones. For example, *p57*, *Irx3*, *BMP10*, and *Cx40* are highly expressed in the trabecular zone, while *Tbx20*, *Hey2* and *N-Myc* are highly expressed in the compact zone (Chen et al., 2004; Kochilas et al., 1999; Sedmera et al., 2000; Zhang et al., 2013). However, the mechanisms underlying the different cardiomyocyte specification between the two zones are unknown.

In order to investigate trabecular morphogenesis and regional specification in mice, we employed the inducible multicolor brainbow system and the embryo clearing system to genetically label, trace, image and analyze cardiomyocytes at single cell level (Hama et al., 2011; Livet et al., 2007; Susaki et al., 2014). The improved imaging depth and scale of the cleared embryos allow for comprehensive 3D reconstruction of the heart and analysis of a single cell with spatial detail at the whole-heart scale. This enables us to determine the cellular dynamics and differentiation of cardiac progenitors *in vivo* during trabeculation. In contrast to zebrafish, in which trabeculation is initiated only by directional migration of cardiomyocytes from the compact zone (Gupta and Poss, 2012; Liu et al., 2010; Peshkovsky et al., 2011; Staudt et al., 2014), we found that in a mammalian system labeled cardiomyocytes undergo either oriented cell division (OCD) or directional migration towards the cardiac lumen, resulting in trabecular formation and regional specification. To further confirm that OCD is required for trabeculation, we disrupted the adherens junctions which are required to establish OCD (den Elzen et al., 2009) by deleting *Cdh2*, the gene encoding N-Cadherin (N-CAD), in the whole heart or in a single labeled cardiomyocyte. Cardiac specific *Cdh2* knockout (CKO) displayed trabeculation defects, and *Cdh2* null clones in a mosaic heart were localized to the heart surface, indicating that both N-CAD dependent OCD and directional migration are required for trabeculation.

To determine whether OCD is an asymmetric cell division that contributes to differential specification between the compact and trabecular zones, we examined the distribution of mRNAs in the dividing cells and the resulting two daughter cells. We found that the mRNAs are not asymmetrically distributed within the dividing cells, but after division, the two daughter cells of a perpendicular OCD display distinct levels of mRNAs. This suggests that the different geometric locations or the different signals that the two daughter cells receive cause the asymmetric levels of mRNAs. This phenomenon is known as an extrinsic asymmetric cell division, and has been well-documented previously in *Drosophila* ovarian stem cells (Knoblich, 2008). We further studied the function of N-CAD in trabecular regional specification, and found that while the *Cdh2* CKO displayed specification defects, the *Cdh2* null clones in a mosaic mouse model did not, indicating that N-CAD does not regulate cell autonomous cardiomyocyte specification.

Materials and Methods

Mouse lines

Mouse lines *Cdh2^{fl/fl}* (Kostetskii et al., 2005), *Rosa26Cre^{ERT2}* (*iCre*) (Badea et al., 2003), *Rosa26-Confetti* (*Conf*) (Livet et al., 2007) and *Rosa26-mTmG* (*mTmG*) (Muzumdar et al., 2007) were purchased from Jackson Lab. Dr. Robert Schwartz provided *Nkx2.5^{Cre/+}* mice (Moses et al., 2001). *iCre* males were crossed with *Conf* and *Cdh2^{fl/fl}*; *Conf* females to generate respectively control clones: *iCre;Conf* and *Cdh2* null clones: *iCre; Conf; Cdh2^{fl/fl}* (*iCdh2*) upon Tamoxifen induction. All animal experiments are approved by the IACUC at Albany Medical College and performed according to the NIH Guide for the Care and Use of Laboratory Animals.

Single mRNA molecule In Situ hybridization and immunofluorescence staining

In Situ hybridization (ISH) and immunofluorescence staining (IFS) were performed according to the protocol of the RNAscope[®] Chromogenic (RED) Assay (Cat. No. 310036), which can detect single mRNA molecules. Briefly, 24 hours after fixation, the embryos were frozen embedded in OCT compound. Sections of the frozen embedded samples were processed following the step-by-step protocol of the kit. The expressional level of mRNA in each cell was based on the number of mRNA molecules or signal intensity using the confocal scanned pictures, and three scanned sections for each cell were quantified. The numbers of mRNA molecules in cells at comparable locations were also quantified.

Statistics

Data is shown as mean \pm standard deviation. An unpaired, two-tailed Student's t-test and chi square test as specified were used for statistical comparison. A chi-squared test was used to compare the division pattern distribution or clonal pattern distribution between control and knockout. A P-value of 0.05 or less was considered statistically significant.

Additional materials and methods are available in the online data supplement.

Results

Imaging a labeled cell inside the cleared heart

Single cell tracing and analysis at the whole heart scale during cardiac development is essential to determine the cellular dynamics and differentiation of cardiac progenitor cells *in vivo*, but is hindered by the lack of depth due to tissue opacity and light scattering. To overcome these obstacles, we adapted a system that can render the heart highly transparent for both illumination and detection: the whole embryo clearing (Fig. 1A and Suppl. Fig. 1A&B) (Hama et al., 2011; Susaki et al., 2014; Wu et al., 2010; Zhao et al., 2014). To distinguish endocardial cells from cardiomyocytes, embryos were stained for the endothelial cell marker PECAM in the far-red channel, and counter-stained with DAPI in the blue channel to identify the geometric location of each cell in the heart. Individual cardiomyocytes inside the cleared heart are visible and can be imaged via confocal microscopy (Fig. 1B). Cell orientation, division patterns, and geometric localization of the labeled cells in the heart can be determined with Imaris software (Fig. 1B and Suppl. Movie 1). To generate single cell clones in a temporally controlled manner, we crossed *iCre* (Badea et al., 2003), whose Cre nuclear localization can be induced by tamoxifen, with the reporter mouse *Conf* (Livet et al., 2007). *Conf* reporter mice in theory can stochastically generate nuclear green, cytoplasmic yellow, cytoplasmic red, or membrane-bound cyan fluorescent protein upon transient Cre mediated recombination in an individual cell (Suppl. 1C&D) (Livet et al., 2007). To determine the timing of labeling, we gavaged pregnant females bearing E7.75 embryos with tamoxifen at a dosage of 20 μg per gram of body weight (20 $\mu\text{g}/\text{g}$). While we did not observe any fluorescent cells 12 hours after induction, after 16 hours individual fluorescent cells were observed in the *iCre; Conf* hearts (Fig. 1C). At a dosage of 20 $\mu\text{g}/\text{g}$, the number of recombinant fluorescent clones in the ventricle 24 hours after induction is not significantly different from the number of clones 72 hours after induction (Fig. 1D), indicating that a single dose of tamoxifen at a concentration of 20 $\mu\text{g}/\text{g}$

or lower does not cause continuous labeling in the heart. To determine the dosage of tamoxifen required to label a single cell of an embryonic heart tube at around E8.0-E8.5, we induced transient Cre activation using different dosages of tamoxifen when the embryos were at E7.75. We quantified the number of recombined clones (recombined blue clones were not quantified due to DAPI staining) per ventricle 72 hours after induction and found that the number of clones in the ventricle was tamoxifen dosage-dependent (Fig. 1E). Tamoxifen at 10 $\mu\text{g/g}$ induced one or no recombination event in the primitive ventricle (Fig. 1E) and was used for the following lineage tracing experiments unless otherwise specified. It is interesting to note that this concentration is higher than the previously reported 4 $\mu\text{g/g}$ that can induce single recombination in the embryonic retina, and the difference might be due to different reporter mouse lines used and different organs examined (Badea et al., 2003). Probabilistic calculations indicated that a dosage of 10 $\mu\text{g/g}$ can be used to induce clonal analysis with a very low risk of adjacent cell labeling, as detailed in Supplemental Data and Suppl. Fig. 2A&B.

Cardiomyocyte clones display four types of geometric patterns

To determine cellular dynamics during trabecular initiation, pregnant females were gavaged with tamoxifen when the embryos were at about E7.75, so that cardiomyocytes would be labeled at E8.0-E8.5, a stage when the myocardium consists of a single cell layer and the trabeculae are not yet initiated (Suppl. Fig. 3A&B). We obtained 286 E10.5 embryos that each contained a single clone in the ventricle. Of them, 67 were endothelial clones (Fig. 2A&C) marked by PECAM staining (Suppl. Movie 2), while 217 were cardiomyocyte clones (Fig. 2A&D-G) (Suppl. Movie 3). Because cardiomyocytes and endocardial cells are already segregated at E8.0-8.5, we only observed two bi-potent clones that contained mostly cardiomyocytes and a few endothelial cells (Data not shown).

72 hours after induction, the labeled single cell had undergone several rounds of cell divisions, and the clones exhibited specific geometric patterns. To better define the geometric patterns, we divided the myocardium into three zones: outer compact, inner compact, and trabecular (Fig. 2B). Based on the geometric distribution and anatomical annotation of each clone, the clones were categorized into four different patterns. In one clonal pattern, cells are localized to outer compact, inner compact and trabecular zones, with one cell of the clone remaining in the outer compact zone (Fig. 2D & Suppl. Movie 3). This type of clone was defined as a transmural clone. The second type, in which all the cells are in the outer compact layer of the myocardium, was defined as a surface clone (Fig. 2E and Suppl. Movie 4). The third type displays two or more cells in the outer compact zone and some cells in the inner compact zone or trabecular zone, and was defined as a mixed clone (Fig. 2F and Suppl. Movie 5). In the fourth type, all the cells are in the inner compact zone and/or trabecular zone, and were defined as an inner clone (Fig. 2G, Suppl. Movie 6). Of the 217 cardiomyocyte clones, 73 (33%) were transmural clones, 62 (29%) were inner clones, 32 (15%) were surface clones, and 50 (23%) were mixed clones (Fig. 2H).

Inner, transmural and mixed clones contribute to trabeculation

We further characterized the clones by quantifying the location, size, and number of cells of each control and *Cdh2* null clone (The *Cdh* null clones will be explained later). Of the four

types of clones, surface clones displayed the shortest depth (z), defined by the length from the heart surface to the cell that is furthest to the surface, while the inner clones invaded the deepest (Fig. 3A). The length and width of the clones (from a surface view) were quantified as x and y to reflect lateral spread, and mixed clones had the largest lateral spread (Fig. 3B&C). We also quantified cell numbers in the different clones and found that surface clones had the lowest, while mixed clones had the highest numbers of cells among the four types (Fig. 3D). Based on the depth and length of x and y in Fig. 3A–C, we drew a schematic model of the four types of clones regarding their contribution to trabeculation (Fig. 3E). The surface clone is localized at the outer compact zone, while the inner clone migrates furthest, with the majority of the inner clones localized inside the inner compact zone or trabecular zone. The transmural clone spans from the outer compact, to the inner compact, and to the trabecular zone, while the cells of the mixed clone usually reside in the outer and inner compact zone with some cells are in the trabecular zone (Fig. 3A&E).

Myocardial cells OCD contributes to different clonal patterns

We hypothesized that the clonal patterns are determined by the mitotic spindle orientation of the initial labeled cell. To determine mitotic spindle orientation of dividing cardiomyocytes during trabecular initiation, E9.0–9.5 *Nkx2.5^{Cre/+}; mTmG* embryos were whole mount stained with antibodies against acetylated α -tubulin and PECAM. We found that the majority of mitotic cells displayed either parallel orientation (40%, n=75) with a spindle angle less than 30 degrees, or perpendicular orientation (52%, n=75) with an angle greater than 60 degrees relative to the heart surface (Fig. 4A&B) (The division patterns of cardiomyocytes in *Cdh2 CKO* will be explained later).

To evaluate the OCD of cardiomyocytes *in vivo*, we examined labeled cardiomyocytes 24 hours after tamoxifen administration using the *iCre;Conf* system and found that within that time frame most labeled cells undergo one round of division to yield two cells (Fig. 4C–E). Since one daughter cell is at the surface of the compact zone, and the other daughter is in the trabecular zone or inner compact zone (Fig. 4C), we infer that the two daughter cells resulted from a perpendicular division. When both daughter cells are in the compact zone, it suggests a parallel division (Fig. 4D). In a migratory clone, the labeled cells migrate away from the outer compact zone into the heart (Fig. 4E) (Staudt et al., 2014). To determine whether the cardiomyocytes can further undergo OCD at later stages, we labeled the cells by gavaging tamoxifen to pregnant females when the embryos were at E8.75, at a concentration of 20 $\mu\text{g/g}$ for 24 hours (Considering that the E8.75 heart contains more cells and clones labeled for 24 hours contain only 1–3 cells, the probability of adjacent labeling with a tamoxifen concentration at 20 $\mu\text{g/g}$ remains low). We found that the percentages of cells labeled at E7.75 and E8.75 that undergo perpendicular division were 43% (n=57) and 40% (n=66) respectively, which is not significantly different.

OCD and directional migration contribute to trabeculation in an N-CAD dependent manner

Previous work has shown that N-CAD, a component of adherens junctions, is essential for trabeculation (Ong et al., 1998). The *Cdh2 CKO* embryos die before E10.5 as previously reported (Luo et al., 2001). A BrdU pulse-labeling assay revealed that *Cdh2* null cardiomyocytes displayed a significantly lower proliferation rate compared to control (data

not shown). *Cdh2* deletion causes cardiomyocytes to be loosely associated (Luo et al., 2001), and some hearts exhibited an absence of trabeculae and an abnormal morphology (Fig. 5A&B), while others contained loose cardiomyocytes within the heart lumen (Data not shown). The mitotic spindle orientation pattern of the CKO cardiomyocytes is significantly different from that of the controls (Fig. 4A&B) ($\chi^2=94.898$, $df=2$, $p<0.0001$), with parallel divisions occurring at a frequency of 37% and perpendicular at 29% ($n=35$) (Fig. 4A&B). However, the random mitotic orientation of CKO cardiomyocytes might be due to cardiac growth arrest, and whether it contributes to the trabeculation defects is not clear. To avoid cardiac growth arrest and further study how N-CAD regulates trabeculation, we labeled and deleted *Cdh2* within individual cells of *iCre; Conf; Cdh2^{fl/fl} (iCdh2)* hearts by inducing Cre activation at E7.75 and examined the clonal patterns and distributions of *iCdh2* clones 72 hours later. The deletion of *Cdh2* within the *iCdh2* null clone was confirmed by N-CAD staining, 78% ($n=23$) of the labeled clones displayed absence of N-CAD (Fig. 5C). We observed that 42% of the *iCdh2* clones are surface clones, 6% are transmural clones, 19% are inner clones, and 33% are mixed clones ($n=128$) (Fig. 5D). These observations are significantly different from the clonal patterns in the controls (Fig. 5D; $\chi^2=147.151$, $df=3$, $p<0.0001$). In addition, the overall geometric location of *iCdh2* clones is different from that of the control clones, as the *iCdh2* clones primarily localized to the heart surface and failed to invade deeply into the heart when compared to control clones (Fig. 5E, Fig. 3A–C and Suppl. Movie 7). Furthermore, unlike the cells in the control clone, which are dispersed (Fig. 2D, F&G), many cells in the *iCdh2* clones are physically connected, suggesting invasion/migration defects (Fig. 5E). The reduced number of transmural, inner and mixed clones, and reduced invasion of all the clones might contribute to the trabeculation defects of the *Cdh2* CKO hearts and indicates that N-CAD regulates trabeculation in a cardiomyocyte autonomous manner. We quantified the number of cells per clone, and found that the clone size of *iCdh2* is significantly smaller than that of the control clones (Fig. 5F).

OCD contributes to trabecular regional specification via a mechanism of extrinsic asymmetric cell division

Trabecular cardiomyocytes are more differentiated than compact cardiomyocytes, although the molecular features and underlying mechanisms of the difference are unknown (Kochilas et al., 1999; Sedmera et al., 2000; Zhang et al., 2013). To determine their distinct specification at an early stage, we adapted an RNAscope ISH/IFS system, in which single mRNAs and certain proteins can be detected simultaneously. We screened several mRNAs including *Bmp10* (Chen et al., 2004), *Hey2* (Koibuchi and Chin, 2007) and *Irx3* (Christoffels et al., 2000), which were previously reported to be differentially expressed in compact and trabecular zones at certain stages, and *Ppib*, which encodes peptidylprolyl isomerase B and is ubiquitously expressed. We found that mRNA of *Hey2* is strongly expressed in compact cardiomyocytes in the left ventricle of an E9.5 heart, but weakly expressed in trabecular cardiomyocytes (Fig. 6A). In contrast, mRNA of *Bmp10* is enriched in trabecular cardiomyocytes of the primitive left ventricle in an E9.5 heart (Fig. 6B). As expected, *Ppib* showed symmetric distribution to compact and trabecular zones (Suppl. Fig. 4A). One potential mechanism contributing to the differential expression of *Hey2* and *Bmp10* in trabecular and compact cardiomyocytes would be the asymmetric distribution of *Hey2* and *Bmp10* in cardiomyocytes that undergo perpendicular OCD. To determine

whether perpendicular OCD contributes to regional specification, E9.5 heart sections were stained with acetylated α -Tubulin and p120 (an adherens junction-associated protein that marks the membrane) and hybridized with probes to *Bmp10* or *Hey2* mRNA. We counted the number of signal dots or signal intensity in dividing cells and quantified the ratio between the two domains of the dividing cell at telophase or the two daughter cells after the division. We found that the mitotic cells undergoing perpendicular divisions did not display asymmetric distribution of *Hey2* (N=8) or *Bmp10* (N=8), as the ratios of *Hey2* or *Bmp10* between the two domains are close to 1 (Fig. 6C, E, I, J and Suppl. Fig. 4B). However, after perpendicular division, when cytokinesis is completed but the two daughter cells are still connected by the midbody, differential *Hey2* and *Bmp10* expression is observed (Fig. 6D, F, I&J and Suppl. Fig. 4C&D). In this type of division, the more luminal daughter cell displays more *Bmp10* and less *Hey2* than the other daughter cell, and the ratio between them for *Hey2* is about 0.5 and for *Bmp10* is about 2 (Fig. 6D, F, I&J and Suppl. Fig. 4C&D). In parallel divisions, the asymmetric distribution of *Hey2* and *BMP10* is not observed (Fig. 6G–I).

As genetic tools to separate trabecular and compact cells are not available, and single cell analysis from the whole tissue via fluidigm cannot include the geometric location of each cell, we used laser capture microdissection to separate trabecular and compact cardiomyocytes. We captured cardiomyocytes separately from the compact zone and trabecular zone in E9.5 hearts and compared the expression profiles of target genes between the compact and trabecular cells. We found that *Hey2* is highly expressed in compact cells, and *BMP10* and *Irx3* are highly expressed in trabecular cells, while expression levels of *Irx4*, *MYH6* and *MYH7* are not significantly different (Fig. 6K), which is consistent with the ISH results (Fig. 6A–J).

N-CAD regulates trabecular regional specification in a cell non-autonomous manner

We examined the mRNA expression patterns of *Hey2* and *Bmp10* in *Cdh2* *CKO* hearts and found the expression of *Hey2* and *Bmp10* in compact and trabecular cardiomyocytes is different from the controls, with trabecular or inner compact zone expressing similar levels of *BMP10* and *Hey2* to the compact zone (Suppl. Fig. 5A&B and Data not shown), indicating a trabecular regional specification defect. The cause of this defect can be cell non-autonomous, such as through disrupted localization to the cardiac jelly, or autonomous. To distinguish these two possibilities, we induced labeling and deleted *Cdh2* in cells of *iCre; Conf; Cdh2^{fl/fl}* hearts by inducing Cre at E7.75 and then tracing for 72 hours. We examined the expression of *Hey2* and *Bmp10* in the *iCdh2* clones. We found that *Bmp10* expression levels in the *iCdh2* clones in the outer compact, inner compact and trabecular zones are different, with lower *Bmp10* expression in the outer compact zone than in the trabecular zone (Suppl. Fig. 5C&D). However, the *Bmp10* levels in *iCdh2* clones of different zones are comparable to those in adjacent control cells (Suppl. Fig. 5C&D), indicating that it is the geometric location of the cell and not the N-CAD deletion that determines the differential *Bmp10* expression. Similarly, *Hey2* expression in *iCdh2* clones in the compact zone is higher than in clones in the trabecular zone, and each clone's expression level is not significantly different from that of the surrounding control cells (Suppl. Fig. 5 E&F). These results indicate that N-CAD regulates the trabecular regional specification cell non-

autonomously by regulating the invasion and migration of cardiomyocytes to different geometric locations where extrinsic signals from cardiac jelly or endocardium may instruct the regional specification.

Discussion

In mammals, it has been described that trabecular morphogenesis involves the recruitment of cells from the compact zone. However, the cues and the mechanisms underlying cardiomyocyte recruitment are unknown. To address these questions, we investigated trabeculation using single cell lineage tracing, clonal mosaic models, and tissue-specific knockout mouse models. Our study demonstrates that early stage cardiomyocytes within the forming compact zone undergo OCD and directional migration via an N-CAD dependent mechanism to contribute to trabeculation. Perpendicular OCD contributes to trabecular morphogenesis, and causes daughter cells to be positioned within different geometric locations in the heart, and exposed to different extracellular signals, resulting in different specification decisions between the two daughter cells.

OCD and directional migration contribute to trabecular initiation is N-CAD dependent

Studies in avian hearts led to the general belief that cardiomyocytes in trabecular and compact myocardium are derived from myocardial progenitor cells that differentiate via local proliferation (Mikawa et al., 1992b; Mikawa and Fischman, 1996). Previous work in zebrafish showed that the myocytes forming the trabeculae arise from a different clonal origin than the cardiomyocytes in the compact zone (Gupta and Poss, 2012; Liu et al., 2010). Conversely, our results demonstrate that trabecular and compact cardiomyocytes within the transmural and mixed clones share the same progenitor cell in the mouse, indicating that at least some compact and trabecular cardiomyocytes arise from a common progenitor cell.

In our single cell lineage tracing study, the existence of four distinct clonal patterns suggests that the labeled cardiomyocytes might undergo OCD or directional migration during trabeculation. Previous work showed that cardiomyocytes at E13.5 undergo primarily parallel OCD based on IFS (Le Garrec et al., 2013), which is consistent with the heart morphogenesis at E13.5, a stage in which trabecular formation is already completed and the heart undergoes expansion. Hence, a high percentage of parallel OCD would be expected. In this study, we found that 52% of cardiomyocytes at E9.0-E9.5, a stage at which the myocardium initiates trabecular formation, undergo perpendicular OCD, consistent with the observed transmural growth of trabeculae. However, the IFS only allows for observation of cell division patterns at a single window in time, and we would expect that prolonged observation such as time lapse imaging and lineage tracing of individual cells might be needed to unveil the cellular dynamics during trabeculation. The daughter cells' relative localizations observed in our single cell lineage tracing for different lengths of time suggest that cardiomyocytes undergo perpendicular OCD during trabeculation (Fig. 4C). Perpendicular OCD allows entry of a daughter cell into the cardiac lumen to initiate trabeculation, thereby leading to the formation of the transmural clone (Fig. 7A&B), which is consistent with previous reports that perpendicular OCD is a polarized cell division and is involved in morphogenesis (Baena-Lopez et al., 2005; Wu et al., 2010). The inner clones

indicate that murine cardiomyocytes might undergo cytoskeletal rearrangement (Fig. 7A&B), become elongated, and migrate toward the heart lumen and contribute to the mass of the trabeculae as previously shown in zebrafish, in which trabeculae are formed by directional migration of cardiomyocytes from the compact zone (Gupta and Poss, 2012; Liu et al., 2010; Peshkovsky et al., 2011; Staudt et al., 2014). The existence of the inner clone is consistent with a recent publication showing that *Mesp1* labeled cells form clones inside the mouse heart (Chabab et al., 2016). Parallel division of cardiomyocytes results in a surface clone, and contributes to the enlargement of the heart (Fig. 4A&D). However, we cannot exclude the other possibilities of how the clonal patterns are formed and how the trabeculae are initiated, and time-lapse imaging of trabecular morphogenesis *in vivo* or *ex vivo* might provide more details.

To study the mechanisms that regulate OCD, *Cdh2* was deleted in whole hearts or single cardiomyocytes. We found that *iCdh2* null clones display abnormal clonal patterns with significantly more surface clones, but fewer transmural clones (Fig. 5D), indicating that N-CAD regulates OCD. Furthermore, cells in transmural, mixed and inner *iCdh2* null clones invade the myocardium less deeply (Fig. 3A–C) and most of the cells of these clones are connected rather than dispersed as in the control (Fig. 5E&2D), indicating that N-CAD is required for cardiomyocyte migration and invasion in addition to establishing OCD (Fig. 7A&B). Consistently, previous reports showed that adherens junctions were essential to establish mitotic spindle orientation in *Drosophila* (Inaba et al., 2010), in mouse epicardial cells (Wu et al., 2010) and multiple stem cells (Lechler, 2012). That N-CAD is required to establish spindle orientation is demonstrated in *in vitro* systems such as MDCK cells and MCF10A cells, as disruption of adherens junctions causes the spindle orientation to be random (den Elzen et al., 2009). The lower proliferation rate of the *Cdh2* null cells results in smaller-sized clones, but would not be expected to contribute to clonal pattern changes; instead, the clonal pattern change might be due to the ability of N-CAD to regulate spindle orientation and directional migration.

During trabecular morphogenesis, the appearances of clones that are labeled at different developmental stages are different. Clones labeled at E6.75 displayed dispersive growth, and the clones displayed several cell clusters at E10.5 examined from the heart surface (Data not shown), consistent with the fragmentation observed before (Lescroart et al., 2014). However, when the cell labeling is induced at E7.75, fragmentation was not observed, indicating that the timing of labeling affects clonal appearances. Another major factor that contributes to the distinct appearances of the clones is the endocardial cell. Initially, the cells of most clones are dispersed rather being closely associated. At about E9.5, the endocardial cells burrow into myocardium, and gradually interact tightly with myocardial cells; this tight interaction forces the cardiomyocytes to integrate and might cause the mixed clone to display a wedge-shape at a later stage (Suppl. Fig. 6A&B), as previously described (Mikawa et al., 1992a). The differential proliferation rates of cardiomyocytes in different regions can also contribute to the different appearances of the clones (Sedmera et al., 2003).

Other factors in the regulation of cardiomyocyte OCD and migration need to be determined to fully understand this process. Possible candidates are signaling pathways or molecules previously found to be required for trabeculation, such as Brg1/ADAMTS1 (Stankunas et

al., 2008), NRG1/ErBb2,4 (Gassmann et al., 1995; Lee et al., 1995; Meyer and Birchmeier, 1995) EphrinB2/EphB4 (Gerety et al., 1999; Wang et al., 1998), BMP10 (Chen et al., 2004), Numb Family Proteins (Wu and Li, 2015; Zhao et al., 2014), Notch signaling (Grego-Bessa et al., 2007), Hand2 (VanDusen et al., 2014), cardiac contraction/hemodynamics (Peshkovsky et al., 2011; Samsa et al., 2015), DAAM1 (Li et al., 2011) and components of the sarcomere and the Z-disk (Finsterer, 2009; Teekakirikul et al., 2013). It will be important to determine whether, and if so how, these players regulate OCD and directional migration.

The potential instructive cues for trabecular regional specification might lie in the cardiac jelly and endocardium

Trabecular cardiomyocytes, which take the major responsibility for pumping at early stages of cardiac development, are more differentiated than compact zone cardiomyocytes (Sedmera et al., 2000). How local proliferation contributes to the distinct differentiation status between compact and trabecular cardiomyocytes remains largely unknown. We discovered that asymmetric expression of *Hey2* and *Bmp10* occurs after but not before cytokinesis in perpendicular OCD, and that the asymmetric expression is due to the differences in geometric location between the two daughter cells, with the one closer to cardiac jelly displaying more *Bmp10* and less *Hey2* compared to the other daughter cell that is relatively closer to the surface of the heart.

Previous work has shown the intercellular signals between the endocardium and myocardium are essential for trabeculation. These signals include Brg1/ADAMTS1, NRG1/ErBb2,4, EphrinB2/EphB4, Notch, Numb Family Proteins, VEGF and angiopoietin. At early stages of trabecular initiation, cardiac jelly separates the endocardium from the myocardium and endocardial cells are not physically connected to myocardial cells in most of the regions. However, it could be possible that certain ligands are secreted to the cardiac jelly to facilitate the interaction between endocardium and myocardium (Lai et al., 2010). At later stages, direct Notch ligand/receptor interaction might be involved in the regulation of trabecular cardiomyocyte differentiation, as recent work has shown that overexpression of glycosyltransferase manic fringe in endocardium can cause abnormal expression pattern of *Hey2* (D'Amato et al., 2016).

Furthermore, disruption of *Has2*, which is responsible for the synthesis of hyaluronic acid, a major component of cardiac jelly, causes abnormal trabecular morphogenesis (Camenisch et al., 2000) (Stankunas et al., 2008), demonstrating the important function of cardiac jelly in trabecular initiation. In addition, *Brg1* in endocardium regulates trabecular morphogenesis by controlling the expression of matrix metalloproteinase ADAMTS1 to modulate cardiac jelly degradation. Our single cell lineage tracing showed that cells from the same clone that occupy different geometric locations with respect to the cardiac jelly show distinct differentiation status, and cells that are adjacent to cardiac jelly display higher *Bmp10* and lower *Hey2* than cells that are close to the heart surface (Suppl. Fig. 7A). The trabecular regional specification defect in *CKO* is not caused by the failure of the *Cdh2* null cells to respond to signaling from the ECM, because the cardiomyocytes in the *Cdh2* null migratory clone display equivalent specification status to the surrounding cells regardless of their proximity to trabecular, compact or inner zones. Rather, the defect seems to reside in the

inability of the *Cdh2* null cells to orient properly in order to migrate toward the cardiac jelly. Based on these data and previous publications (Chen et al., 2013; D'Amato et al., 2016; Grego-Bessa et al., 2007; Lee et al., 1995; Luxan et al., 2013; Meyer and Birchmeier, 1995; Sedmera et al., 2000; VanDusen et al., 2014), it is clear that cues from cardiac jelly and endocardium play an instructive role in cardiomyocyte differentiation (Fig. 7C). However, more work will need to be done to reveal the specific cues and signaling pathways that regulate this trabecular specification process. The high relevance of trabeculation defects to human disease warrants future research in the field.

Supplementary Material

Refer to Web version on PubMed Central for supplementary material.

Acknowledgments

We thank the Wu laboratory members for scientific discussion, Dr. Eric N. Olson for insightful comments, Drs. John Schwartz for critical reading, Saiyang Hu and Yangyang Lu for their technical supports, and Drs. Joseph Mazurkiewicz and Margarida Barroso for help in imaging.

Sources of Funding

This work is supported by AHA [13SDG16920099] and by National Heart, Lung, and Blood Institute grants [R01HL121700] to M.W. A.P. was supported by an R01 grant HL104251. H.A.S. was supported by an R01 grant HLR01092510.

Reference

- Badea TC, Wang Y, Nathans J. A noninvasive genetic/pharmacologic strategy for visualizing cell morphology and clonal relationships in the mouse. *J Neurosci.* 2003; 23:2314–2322. [PubMed: 12657690]
- Baena-Lopez LA, Baonza A, Garcia-Bellido A. The orientation of cell divisions determines the shape of *Drosophila* organs. *Curr Biol.* 2005; 15:1640–1644. [PubMed: 16169485]
- Breckenridge RA, Anderson RH, Elliott PM. Isolated left ventricular noncompaction: the case for abnormal myocardial development. *Cardiol Young.* 2007; 17:124–129. [PubMed: 17319979]
- Camenisch TD, Spicer AP, Brehm-Gibson T, Biesterfeldt J, Augustine ML, Calabro A Jr, Kubalak S, Klewer SE, McDonald JA. Disruption of hyaluronan synthase-2 abrogates normal cardiac morphogenesis and hyaluronan-mediated transformation of epithelium to mesenchyme. *J Clin Invest.* 2000; 106:349–360. [PubMed: 10930438]
- Chabab S, Lescroart F, Rulands S, Mathiah N, Simons BD, Blanpain C. Uncovering the Number and Clonal Dynamics of *Mesp1* Progenitors during Heart Morphogenesis. *Cell reports.* 2016; 14:1–10. [PubMed: 26725109]
- Chen H, Shi S, Acosta L, Li W, Lu J, Bao S, Chen Z, Yang Z, Schneider MD, Chien KR, et al. BMP10 is essential for maintaining cardiac growth during murine cardiogenesis. *Development.* 2004; 131:2219–2231. [PubMed: 15073151]
- Chen H, Zhang W, Sun X, Yoshimoto M, Chen Z, Zhu W, Liu J, Shen Y, Yong W, Li D, et al. *Fkbp1a* controls ventricular myocardium trabeculation and compaction by regulating endocardial *Notch1* activity. *Development.* 2013; 140:1946–1957. [PubMed: 23571217]
- Christoffels VM, Keijsers AG, Houweling AC, Clout DE, Moorman AF. Patterning the embryonic heart: identification of five mouse Iroquois homeobox genes in the developing heart. *Dev Biol.* 2000; 224:263–274. [PubMed: 10926765]
- D'Amato G, Luxan G, Del Monte-Nieto G, Martinez-Poveda B, Torroja C, Walter W, Bochter MS, Benedito R, Cole S, Martinez F, et al. Sequential *Notch* activation regulates ventricular chamber development. *Nat Cell Biol.* 2016; 18:7–20. [PubMed: 26641715]

- den Elzen N, Buttery CV, Maddugoda MP, Ren G, Yap AS. Cadherin adhesion receptors orient the mitotic spindle during symmetric cell division in mammalian epithelia. *Molecular biology of the cell*. 2009; 20:3740–3750. [PubMed: 19553471]
- Devine WP, Wythe JD, George M, Koshiba-Takeuchi K, Bruneau BG. Early patterning and specification of cardiac progenitors in gastrulating mesoderm. *eLife*. 2014;3.
- Finsterer J. Cardiogenetics, neurogenetics, and pathogenetics of left ventricular hypertrabeculation/noncompaction. *Pediatr Cardiol*. 2009; 30:659–681. [PubMed: 19184181]
- Finsterer J. Left ventricular non-compaction and its cardiac and neurologic implications. *Heart failure reviews*. 2010; 15:589–603. [PubMed: 20549343]
- Gassmann M, Casagrande F, Orioli D, Simon H, Lai C, Klein R, Lemke G. Aberrant neural and cardiac development in mice lacking the ErbB4 neuregulin receptor. *Nature*. 1995; 378:390–394. [PubMed: 7477376]
- Gerety SS, Wang HU, Chen ZF, Anderson DJ. Symmetrical mutant phenotypes of the receptor EphB4 and its specific transmembrane ligand ephrin-B2 in cardiovascular development. *Mol Cell*. 1999; 4:403–414. [PubMed: 10518221]
- Grego-Bessa J, Luna-Zurita L, del Monte G, Bolos V, Melgar P, Arandilla A, Garratt AN, Zang H, Mukoyama YS, Chen H, et al. Notch signaling is essential for ventricular chamber development. *Dev Cell*. 2007; 12:415–429. [PubMed: 17336907]
- Gupta V, Poss KD. Clonally dominant cardiomyocytes direct heart morphogenesis. *Nature*. 2012; 484:479–484. [PubMed: 22538609]
- Hama H, Kurokawa H, Kawano H, Ando R, Shimogori T, Noda H, Fukami K, Sakaue-Sawano A, Miyawaki A. Scale: a chemical approach for fluorescence imaging and reconstruction of transparent mouse brain. *Nat Neurosci*. 2011; 14:1481–1488. [PubMed: 21878933]
- Inaba M, Yuan H, Salzman V, Fuller MT, Yamashita YM. E-cadherin is required for centrosome and spindle orientation in *Drosophila* male germline stem cells. *PLoS One*. 2010; 5:e12473. [PubMed: 20824213]
- Jenni R, Rojas J, Oechslin E. Isolated noncompaction of the myocardium. *N Engl J Med*. 1999; 340:966–967. [PubMed: 10094647]
- Knoblich JA. Mechanisms of asymmetric stem cell division. *Cell*. 2008; 132:583–597. [PubMed: 18295577]
- Kochilas LK, Li J, Jin F, Buck CA, Epstein JA. p57Kip2 expression is enhanced during mid-cardiac murine development and is restricted to trabecular myocardium. *Pediatr Res*. 1999; 45:635–642. [PubMed: 10231856]
- Koibuchi N, Chin MT. CHF1/Hey2 plays a pivotal role in left ventricular maturation through suppression of ectopic atrial gene expression. *Circ Res*. 2007; 100:850–855. [PubMed: 17332425]
- Kostetskii I, Li J, Xiong Y, Zhou R, Ferrari VA, Patel VV, Molkentin JD, Radice GL. Induced deletion of the N-cadherin gene in the heart leads to dissolution of the intercalated disc structure. *Circ Res*. 2005; 96:346–354. [PubMed: 15662031]
- Lai D, Liu X, Forrai A, Wolstein O, Michalicek J, Ahmed I, Garratt AN, Birchmeier C, Zhou M, Hartley L, et al. Neuregulin 1 sustains the gene regulatory network in both trabecular and nontrabecular myocardium. *Circ Res*. 2010; 107:715–727. [PubMed: 20651287]
- Le Garrec JF, Ragni CV, Pop S, Dufour A, Olivo-Marin JC, Buckingham ME, Meilhac SM. Quantitative analysis of polarity in 3D reveals local cell coordination in the embryonic mouse heart. *Development*. 2013; 140:395–404. [PubMed: 23250213]
- Lechler T. Adherens junctions and stem cells. *Sub-cellular biochemistry*. 2012; 60:359–377. [PubMed: 22674079]
- Lee KF, Simon H, Chen H, Bates B, Hung MC, Hauser C. Requirement for neuregulin receptor erbB2 in neural and cardiac development. *Nature*. 1995; 378:394–398. [PubMed: 7477377]
- Lescroart F, Chabab S, Lin X, Rulands S, Paulissen C, Rodolosse A, Auer H, Achouri Y, Dubois C, Bondue A, et al. Early lineage restriction in temporally distinct populations of *Mesp1* progenitors during mammalian heart development. *Nat Cell Biol*. 2014; 16:829–840. [PubMed: 25150979]
- Li D, Hallett MA, Zhu W, Rubart M, Liu Y, Yang Z, Chen H, Haneline LS, Chan RJ, Schwartz RJ, et al. Dishevelled-associated activator of morphogenesis 1 (*Daam1*) is required for heart morphogenesis. *Development*. 2011; 138:303–315. [PubMed: 21177343]

- Liu J, Bressan M, Hassel D, Huisken J, Staudt D, Kikuchi K, Poss KD, Mikawa T, Stainier DY. A dual role for ErbB2 signaling in cardiac trabeculation. *Development*. 2010; 137:3867–3875. [PubMed: 20978078]
- Livet J, Weissman TA, Kang H, Draft RW, Lu J, Bennis RA, Sanes JR, Lichtman JW. Transgenic strategies for combinatorial expression of fluorescent proteins in the nervous system. *Nature*. 2007; 450:56–62. [PubMed: 17972876]
- Luo Y, Ferreira-Cornwell M, Baldwin H, Kostetskii I, Lenox J, Lieberman M, Radice G. Rescuing the N-cadherin knockout by cardiac-specific expression of N- or E-cadherin. *Development*. 2001; 128:459–469. [PubMed: 11171330]
- Luxan G, Casanova JC, Martinez-Poveda B, Prados B, D'Amato G, MacGrogan D, Gonzalez-Rajal A, Dobarro D, Torroja C, Martinez F, et al. Mutations in the NOTCH pathway regulator MIB1 cause left ventricular noncompaction cardiomyopathy. *Nat Med*. 2013; 19:193–201. [PubMed: 23314057]
- Meilhac SM, Esner M, Kerszberg M, Moss JE, Buckingham ME. Oriented clonal cell growth in the developing mouse myocardium underlies cardiac morphogenesis. *J Cell Biol*. 2004; 164:97–109. [PubMed: 14709543]
- Meilhac SM, Kelly RG, Rocancourt D, Eloy-Trinquet S, Nicolas JF, Buckingham ME. A retrospective clonal analysis of the myocardium reveals two phases of clonal growth in the developing mouse heart. *Development*. 2003; 130:3877–3889. [PubMed: 12835402]
- Meyer D, Birchmeier C. Multiple essential functions of neuregulin in development. *Nature*. 1995; 378:386–390. [PubMed: 7477375]
- Mikawa T, Borisov A, Brown AM, Fischman DA. Clonal analysis of cardiac morphogenesis in the chicken embryo using a replication-defective retrovirus: I. Formation of the ventricular myocardium. *Dev Dyn*. 1992a; 193:11–23. [PubMed: 1540702]
- Mikawa T, Cohen-Gould L, Fischman DA. Clonal analysis of cardiac morphogenesis in the chicken embryo using a replication-defective retrovirus. III. Polyclonal origin of adjacent ventricular myocytes. *Dev Dyn*. 1992b; 195:133–141. [PubMed: 1297456]
- Mikawa T, Fischman DA. The polyclonal origin of myocyte lineages. *Annu Rev Physiol*. 1996; 58:509–521. [PubMed: 8815805]
- Moses KA, DeMayo F, Braun RM, Reecy JL, Schwartz RJ. Embryonic expression of an Nkx2-5/Cre gene using ROSA26 reporter mice. *Genesis*. 2001; 31:176–180. [PubMed: 11783008]
- Muzumdar MD, Tasic B, Miyamichi K, Li L, Luo L. A global double-fluorescent Cre reporter mouse. *Genesis*. 2007; 45:593–605. [PubMed: 17868096]
- Ong LL, Kim N, Mima T, Cohen-Gould L, Mikawa T. Trabecular myocytes of the embryonic heart require N-cadherin for migratory unit identity. *Dev Biol*. 1998; 193:1–9. [PubMed: 9466883]
- Peshkovsky C, Totong R, Yelon D. Dependence of cardiac trabeculation on neuregulin signaling and blood flow in zebrafish. *Dev Dyn*. 2011; 240:446–456. [PubMed: 21246662]
- Pignatelli RH, McMahon CJ, Dreyer WJ, Denfield SW, Price J, Belmont JW, Craigen WJ, Wu J, El Said H, Bezold LI, et al. Clinical characterization of left ventricular noncompaction in children: a relatively common form of cardiomyopathy. *Circulation*. 2003; 108:2672–2678. [PubMed: 14623814]
- Samsa LA, Givens C, Tzima E, Stainier DY, Qian L, Liu J. Cardiac contraction activates endocardial Notch signaling to modulate chamber maturation in zebrafish. *Development*. 2015; 142:4080–4091. [PubMed: 26628092]
- Sedmera D, Pexieder T, Vuillemin M, Thompson RP, Anderson RH. Developmental patterning of the myocardium. *Anat Rec*. 2000; 258:319–337. [PubMed: 10737851]
- Sedmera D, Reckova M, DeAlmeida A, Coppen SR, Kubalak SW, Gourdie RG, Thompson RP. Spatiotemporal pattern of commitment to slowed proliferation in the embryonic mouse heart indicates progressive differentiation of the cardiac conduction system. *Anat Rec A Discov Mol Cell Evol Biol*. 2003; 274:773–777. [PubMed: 12923887]
- Sedmera D, Thomas PS. Trabeculation in the embryonic heart. *Bioessays*. 1996; 18:607. [PubMed: 8757939]

- Stankunas K, Hang CT, Tsun ZY, Chen H, Lee NV, Wu JI, Shang C, Bayle JH, Shou W, Iruela-Arispe ML, et al. Endocardial Brg1 represses ADAMTS1 to maintain the microenvironment for myocardial morphogenesis. *Dev Cell*. 2008; 14:298–311. [PubMed: 18267097]
- Staudt DW, Liu J, Thorn KS, Stuurman N, Liebling M, Stainier DY. High-resolution imaging of cardiomyocyte behavior reveals two distinct steps in ventricular trabeculation. *Development*. 2014; 141:585–593. [PubMed: 24401373]
- Susaki EA, Tainaka K, Perrin D, Kishino F, Tawara T, Watanabe TM, Yokoyama C, Onoe H, Eguchi M, Yamaguchi S, et al. Whole-brain imaging with single-cell resolution using chemical cocktails and computational analysis. *Cell*. 2014; 157:726–739. [PubMed: 24746791]
- Teekakirikul P, Kelly MA, Rehm HL, Lakdawala NK, Funke BH. Inherited cardiomyopathies: molecular genetics and clinical genetic testing in the postgenomic era. *The Journal of molecular diagnostics : JMD*. 2013; 15:158–170. [PubMed: 23274168]
- Towbin JA, Lorts A, Jefferies JL. Left ventricular non-compaction cardiomyopathy. *Lancet*. 2015
- VanDusen NJ, Casanovas J, Vincentz JW, Firulli BA, Osterwalder M, Lopez-Rios J, Zeller R, Zhou B, Grego-Bessa J, De La Pompa JL, et al. Hand2 is an essential regulator for two Notch-dependent functions within the embryonic endocardium. *Cell reports*. 2014; 9:2071–2083. [PubMed: 25497097]
- Wang HU, Chen ZF, Anderson DJ. Molecular distinction and angiogenic interaction between embryonic arteries and veins revealed by ephrin-B2 and its receptor Eph-B4. *Cell*. 1998; 93:741–753. [PubMed: 9630219]
- Weiford BC, Subbarao VD, Mulhern KM. Noncompaction of the ventricular myocardium. *Circulation*. 2004; 109:2965–2971. [PubMed: 15210614]
- Wu M, Li J. Numb family proteins: novel players in cardiac morphogenesis and cardiac progenitor cell differentiation. *Biomolecular concepts*. 2015; 6:137–148. [PubMed: 25883210]
- Wu M, Smith CL, Hall JA, Lee I, Luby-Phelps K, Tallquist MD. Epicardial spindle orientation controls cell entry into the myocardium. *Dev Cell*. 2010; 19:114–125. [PubMed: 20643355]
- Zhang W, Chen H, Qu X, Chang CP, Shou W. Molecular mechanism of ventricular trabeculation/compaction and the pathogenesis of the left ventricular noncompaction cardiomyopathy (LVNC). *Am J Med Genet C Semin Med Genet*. 2013; 163:144–156. [PubMed: 23843320]
- Zhao C, Guo H, Li J, Myint T, Pittman W, Yang L, Zhong W, Schwartz RJ, Schwarz JJ, Singer HA, et al. Numb family proteins are essential for cardiac morphogenesis and progenitor differentiation. *Development*. 2014; 141:281–295. [PubMed: 24335256]

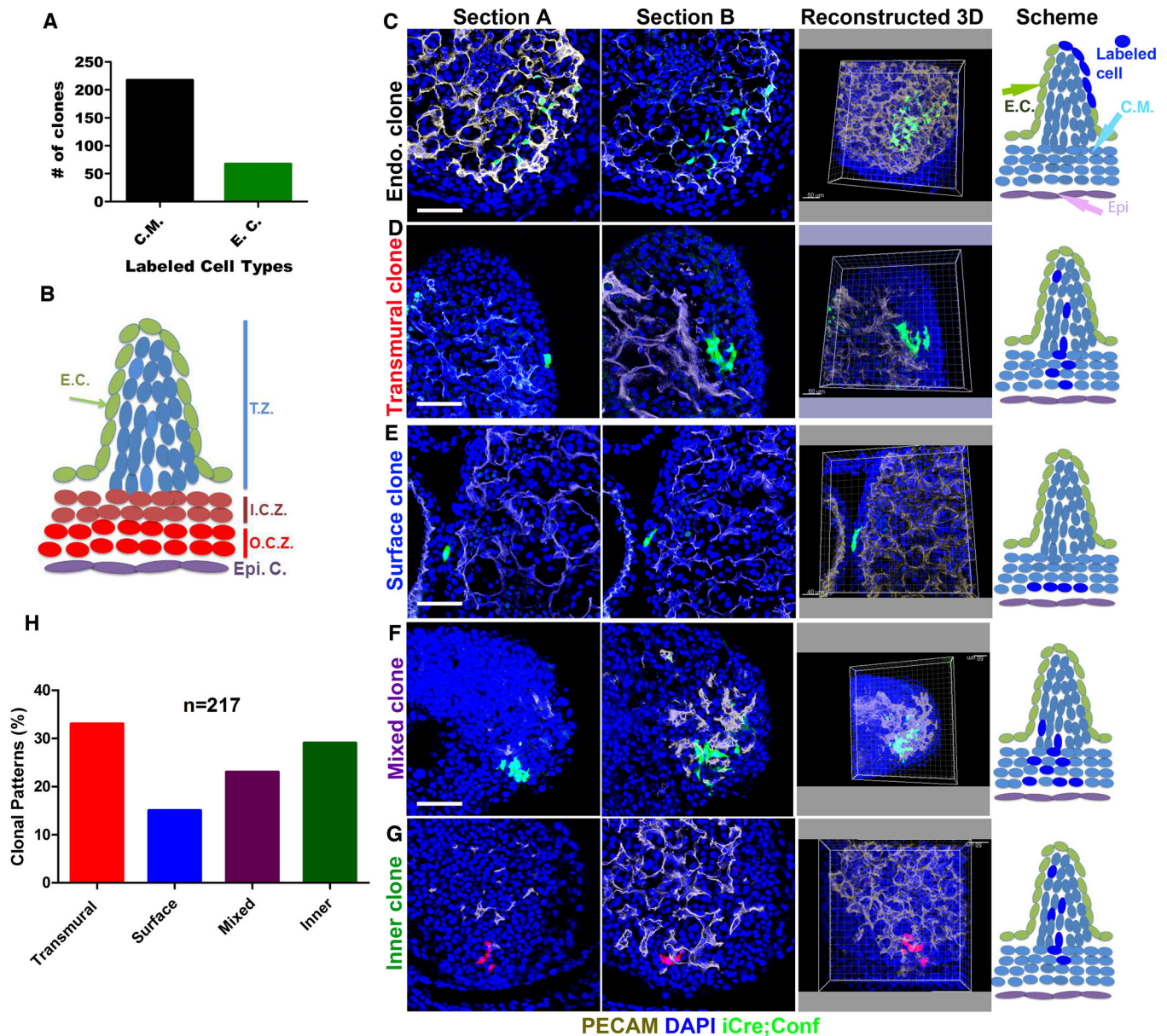


Figure 2. The labeled clones display four types of geometric patterns
 (A) The number of clones of each cardiac cell type was identified. (B) The different zones of the heart were schematically defined, including O.C.Z. (Outer compact zone), I.C.Z. (Inner compact zone) and T.Z. (Trabecular zone). (C–G) Sections A & B are two representative sections from a Z stack of the same clone. The Z stack was reconstructed to a 3D image. Scheme is an illustration to show the geometric pattern of the clone. (C) An endocardial cell clone. (D) A transmural clone. (E) A surface clone. (F) A mixed clone. (G) An inner clone. (H) shows the percentage distribution of different types of clones. E.C.: endocardial cells; C.M.: cardiomyocytes; Epi: epicardial cells. Scale bars in C–G are 50 μ m.

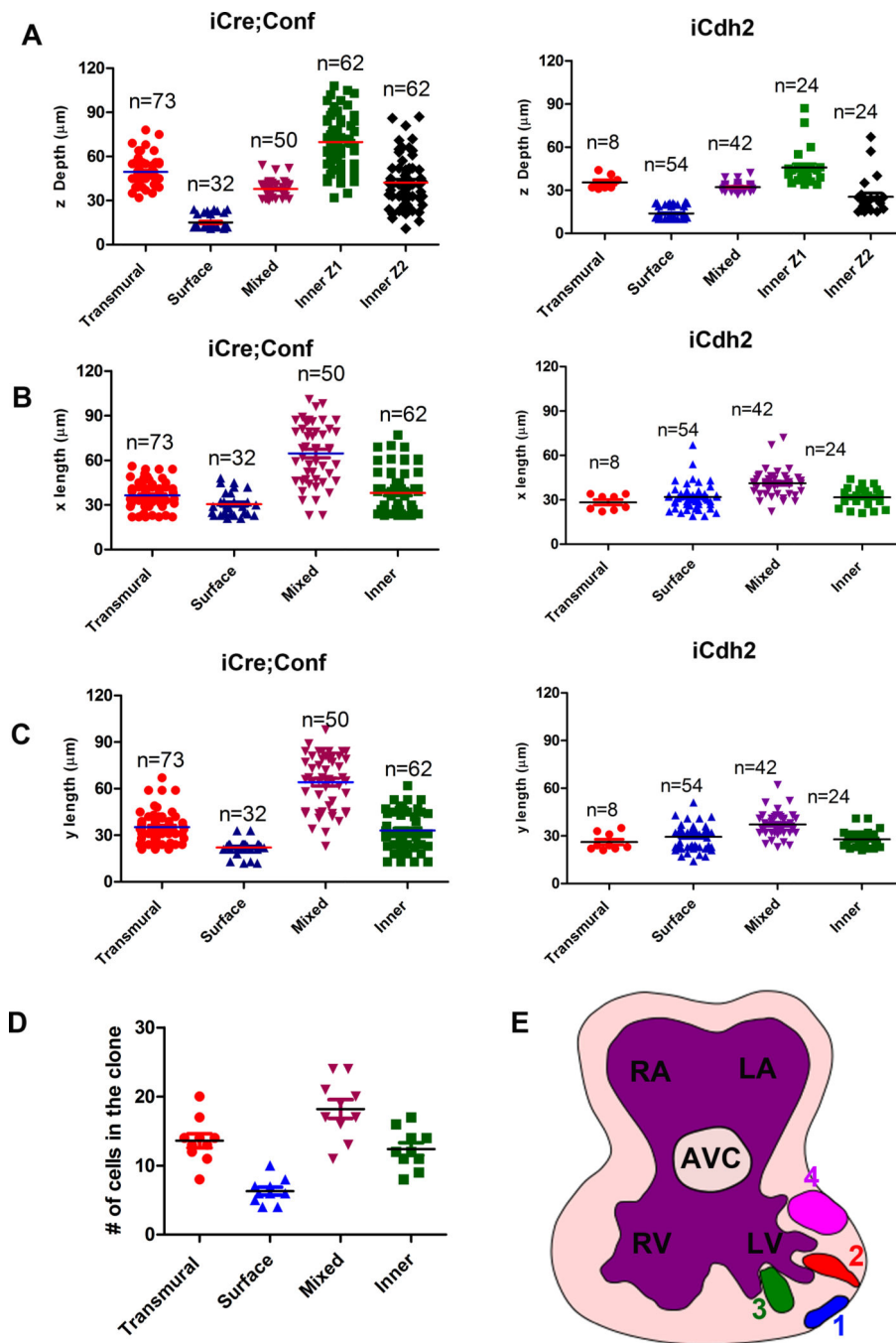


Figure 3. Inner and transmural clones contribute to trabeculation

(A–C) Comparison of the values of x, y and z in different types of clones between control and *iCdh2* null clones. z is the depth from the heart surface to the cell that is the furthest away from the heart surface, and x and y are the lengths the clone spans in the x and y axis, respectively. For the inner clone, z1 and z2 are respectively the distances of the furthest cell and the closest cells to the heart surface. (D) Shows the number of cells in 4 different types of control clones. 10 clones from each type were presented. (E) The distribution of the 4 control clones: 1, surface clone; 2, transmural clone; 3, inner clone; and 4, mixed clone in

the heart. RV: right ventricle; LV: left ventricle; RA: right atrium; LA: Left atrium. AVC: atria-ventricular cushion.

Author Manuscript

Author Manuscript

Author Manuscript

Author Manuscript

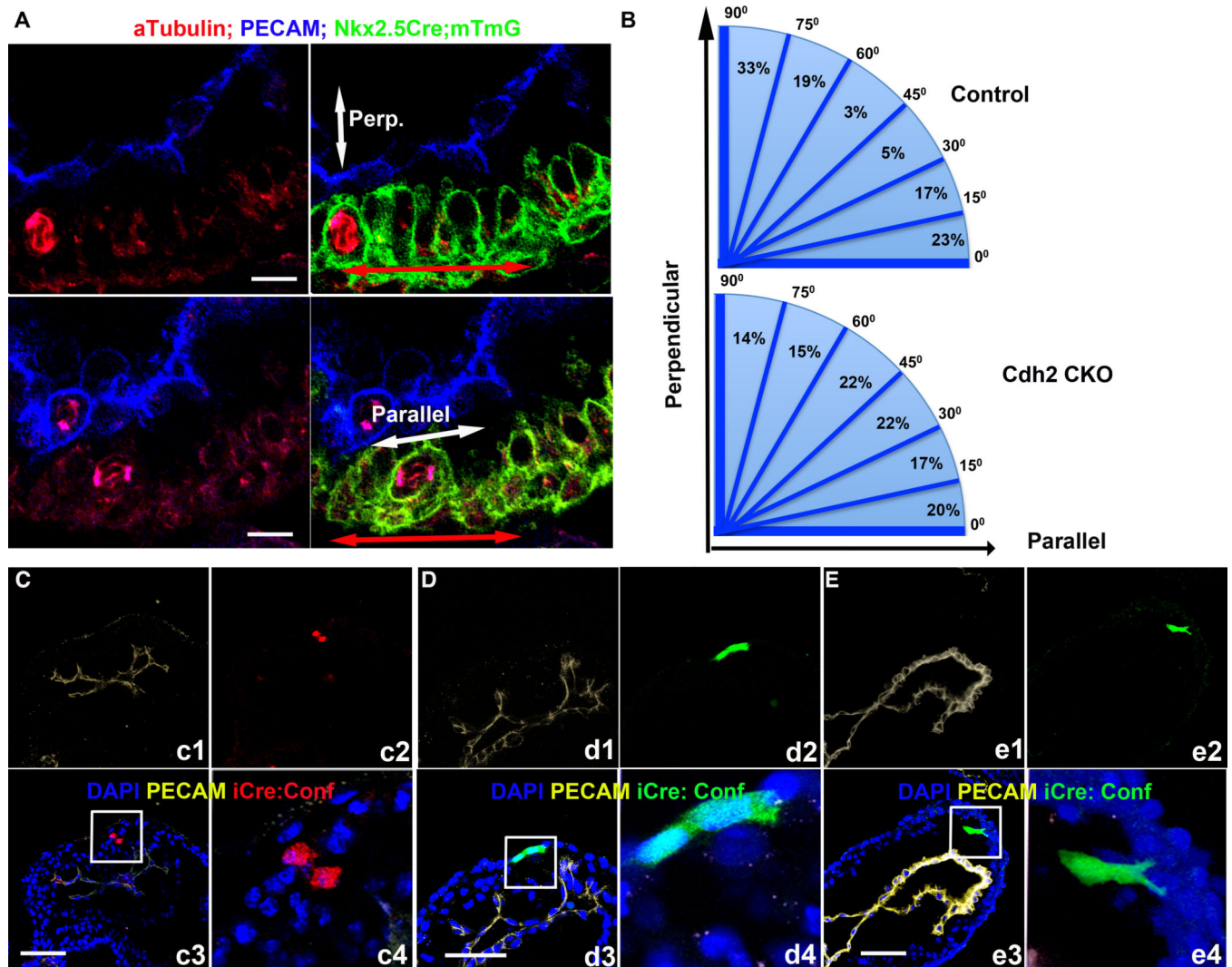


Figure 4. Myocardial cells undergo parallel and perpendicular divisions

(A) E9.0-9.5 hearts were whole mount stained with acetylated α -tubulin and PECAM. Images show that cardiomyocytes undergo perpendicular (perp.) and parallel divisions. (B) The mitotic spindle orientation patterns of cardiomyocytes from control and *Cdh2 CKO* at E9.0-E9.5 hearts. The horizontal line represents the axis of heart surface and the each blue line represents an angle between mitotic spindle and heart surface. The number between blue lines indicates the percentage of cells whose mitotic spindle angle is between the two angles represented by the blue lines. (C–E) *iCre; Conf* embryos were induced with tamoxifen at E7.75 and were examined 24 hours after induction. The labeled cells could undergo perpendicular division (C), parallel division (D), and directional migration (E). There are four quadrants in C–E. c1, d1 and e1 are the PECAM staining; c2, d2 and e2 show the fluorescent protein; c3, d3 and e3 show the merged pictures; and c4, d4 and e4 show the enlarged quadrant in c3, d3, and e3, respectively. Scale bar in A is 10 μ m and in C–E are 50 μ m.

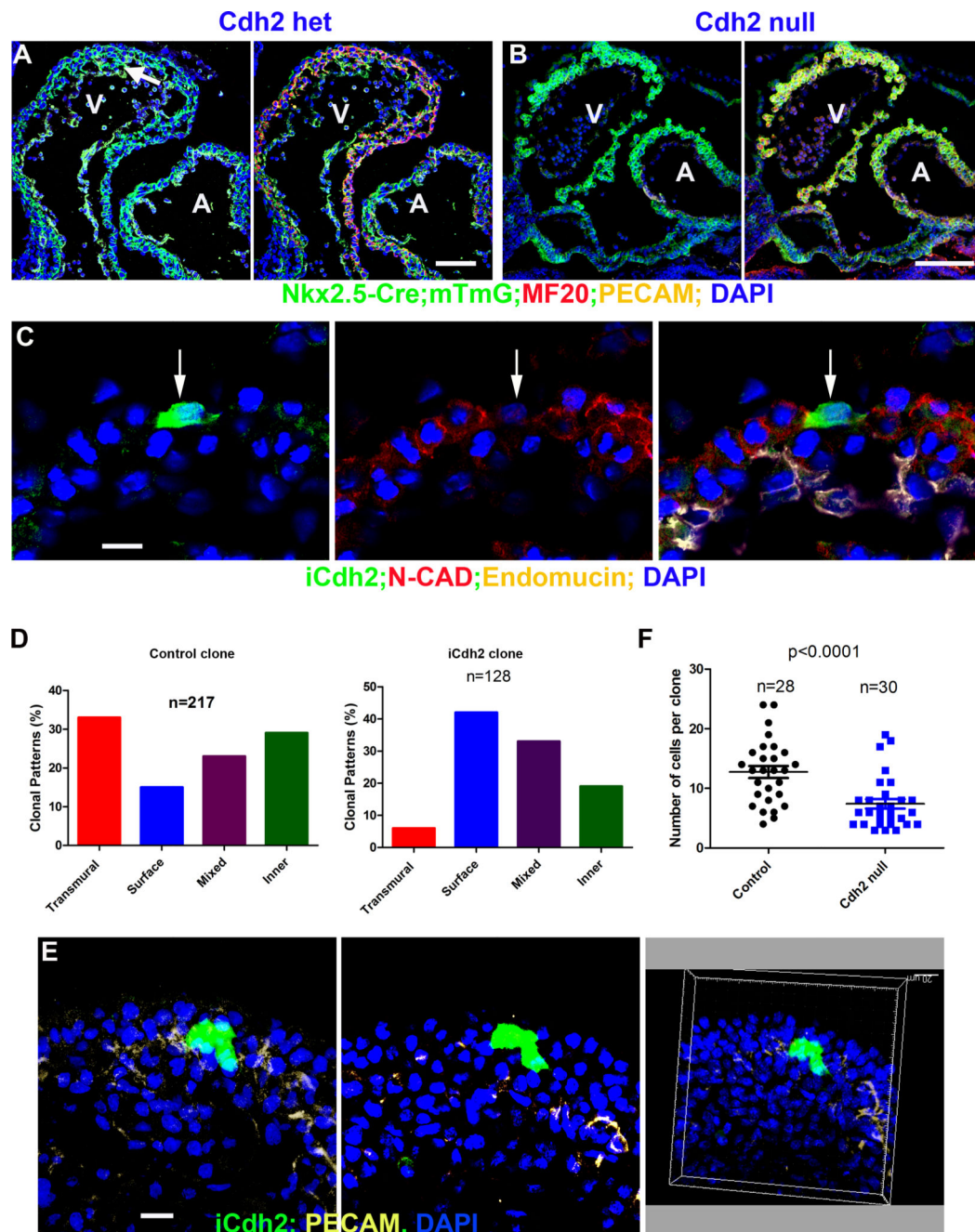


Figure 5. OCD and directional migration contribute to trabeculation in an N-CAD dependent manner

(A–B) show sagittal sections of *Cdh2* heterozygous or *CKO* hearts at E9.5. Arrow points to a trabecula. (C) N-CAD was not detected in *iCdh2* clone indicated by an arrow. (D&E) show the clonal patterns of control and *iCdh2*. The control is the same as Fig. 2H. (E) Cells in the *iCdh2* were not dispersed. Pictures show two sections from a Z stack and a reconstructed 3D picture. (F) The clonal sizes of *iCdh2* clones are significantly smaller than the control. Scale bars in A–B are 100 μ m and in C&E 10 μ m. A: atrium; V: ventricle.

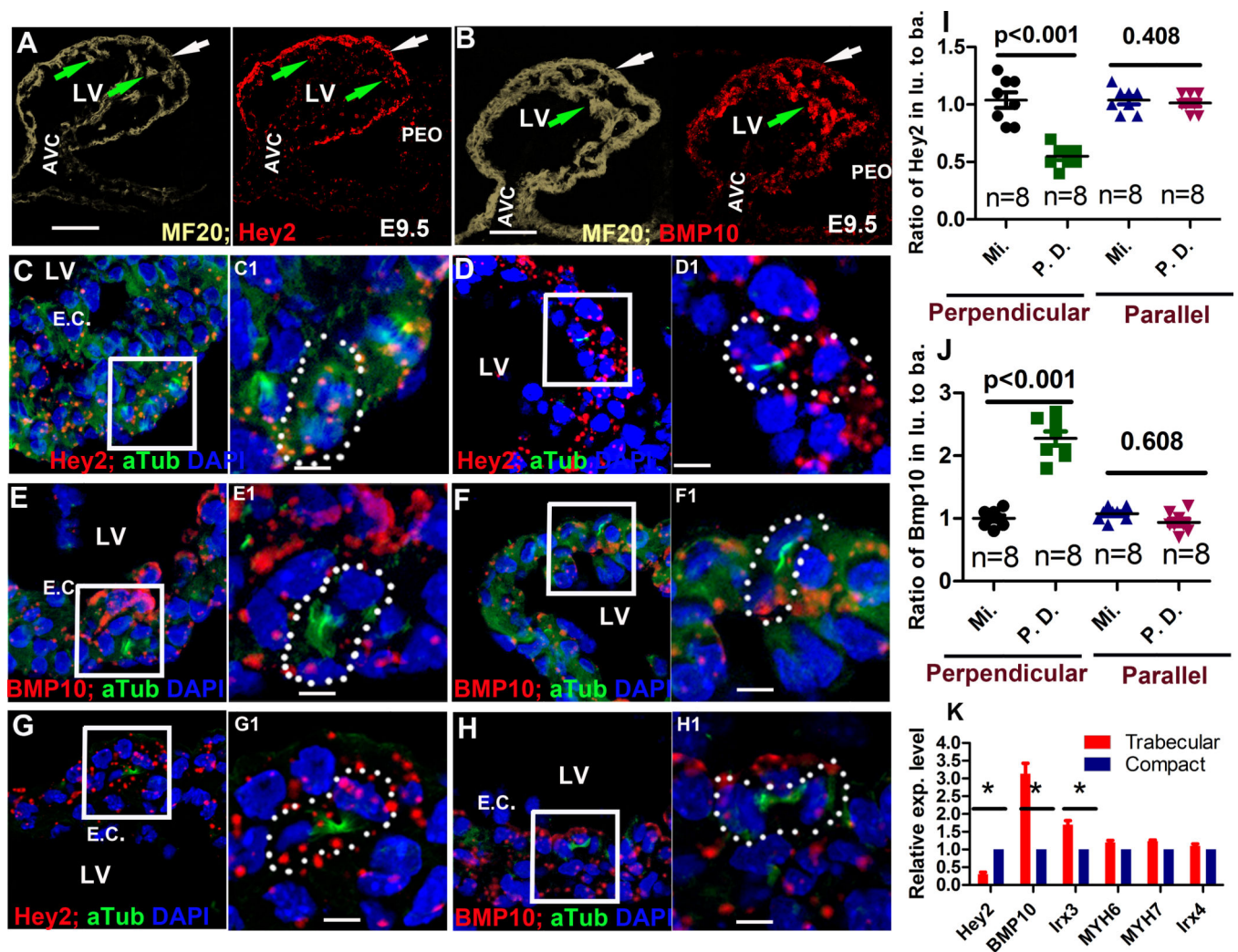


Figure 6. Extrinsic asymmetric cell division might contribute to asymmetric expression of Hey2 and BMP10 in trabecular and compact zones

(A–B) *Hey2* and *BMP10* are asymmetrically distributed to compact and trabecular zones with *Hey2* enriched in the compact zone (A) and *BMP10* enriched in the trabecular zone (B). (C–H) All show one low magnification picture to the left and one section of the same cells with higher magnification on the right. (C) *Hey2* and (E) *BMP10* are not asymmetrically distributed in perpendicular dividing cells. After division, when the two daughter cells are separated but still connected at the mid-body, both (D) *Hey2* and (F) *BMP10* are asymmetrically distributed, with the daughter closer to cardiac jelly displaying less *Hey2* and more *BMP10* than the daughter at the heart surface. In parallel division, both *Bmp10* and *Hey2* are symmetrically distributed (G&H) to the two daughter cells. (I&J) shows the ratio of *Hey2* and *BMP10* between the twodomains/ daughter cells in perpendicular/parallel mitotic or post-division cells (Three sections for each cell and n=8 for each type). (K) Q-PCR data to show the differential expression between trabecular and compact cardiomyocytes harvested by LCM of an E9.5 heart. The experiments were repeated three times. Scale bars in A&B are 100 μ m and in C–H 10 μ m. Lu: luminal; ba:

basal; Mi: mitotic; P.D.: post-division. E.C.: Endocardial cells; LV: left ventricle; AVC: atrioventricular canal; PEO: pro-epicardial organ.

Author Manuscript

Author Manuscript

Author Manuscript

Author Manuscript

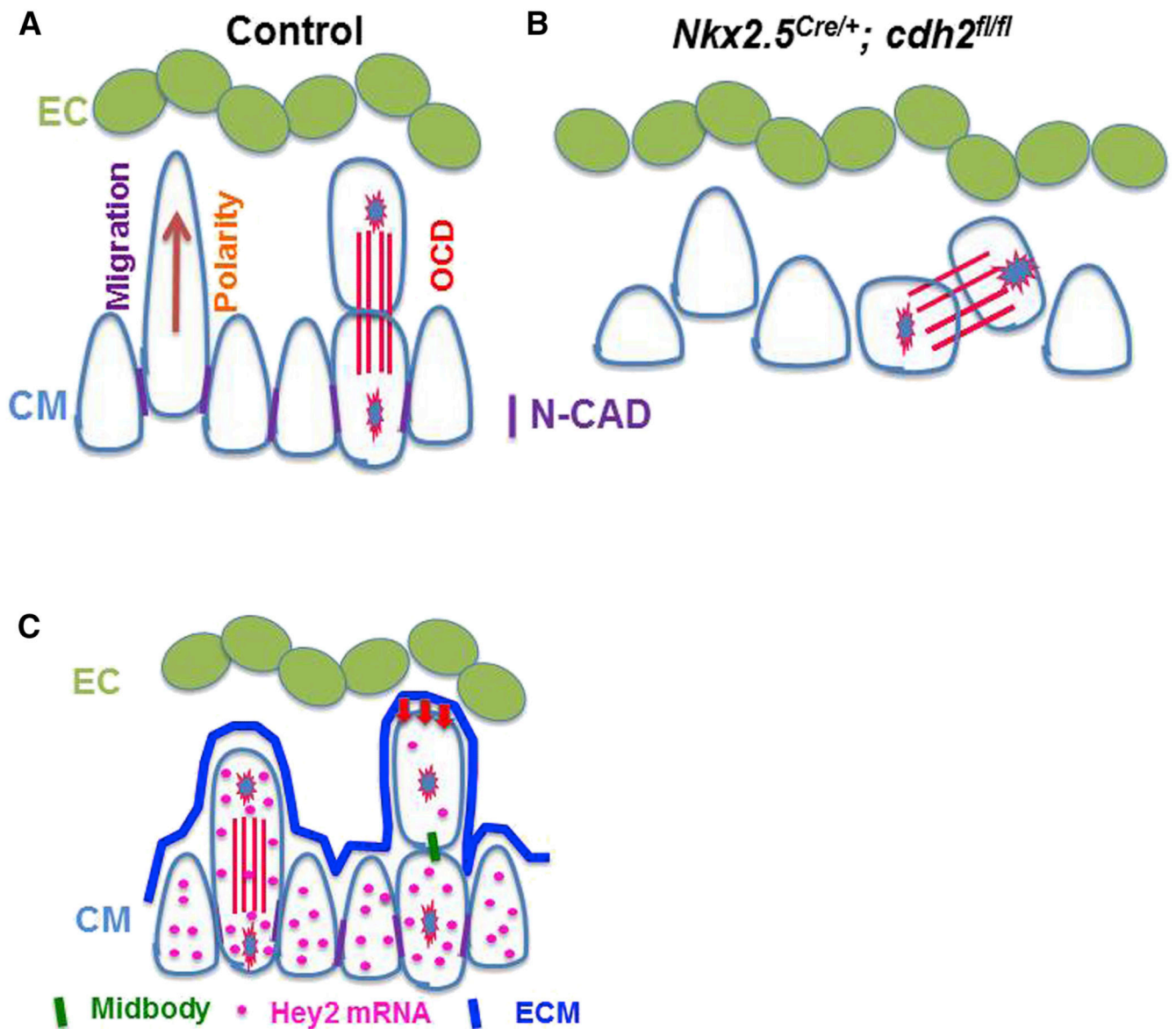


Figure 7. Models of trabecular initiation and trabecular regional specification

(A&B) OCD and directional migration contribute to trabecular initiation in an N-CAD dependent manner. *Cdh2 null* cells failed to undergo OCD and directional migration. (C) Cardiac jelly and endocardium might provide instructive cues for trabecular regional specification.